

Fracture mechanism of plant fibres

E. C. McLAUGHLIN

*Department of Physics, University of the West Indies (UWI),
Kingston 7, Jamaica, W. Indies*

R. A. TAIT

*Department of Mechanical Engineering, University of Houston, Houston,
Texas 77004, USA*

This paper, which describes work from an extensive study of various plant species, is aimed at presenting the best common physical description of the mechanism of failure in tension of cellulose-based fibres. A correlation coefficient of $r = 0.69$ was observed between the mean tensile strengths and Young's moduli of fibres extracted from leaves, stems, and other miscellaneous sources. This observation is attributed to increases in Young's modulus and tensile strength with decreasing microfibril angle and increasing cellulose content. A cylindrical cell model was applied to the mean tensile strengths of fibres preconditioned at 24 to 27°C and 60% relative humidity. A modification of the resulting expression was used to produce the best correlation coefficient of $r = 0.89$ between predicted and measured mean tensile strengths. However, the importance of cellulose content for strength which is presently illustrated for various plant species is not reflected in terms of mean fracture strain, which was increased by increasing microfibril angle showing why high works of fracture can be obtained from different species.

1. Introduction

A common failure mode featuring the uncoiling of cellulose microfibrils within fibres from different plant sources has been identified. Evidence reported by Jeronimidis [1] for timber, and by McLaughlin and Tait [2] for *Sansevieria metallica* show that works of fracture were as high as 10^5 J m^{-2} . Furthermore, an example of the decrease in Young's modulus (E) with microfibril angle (θ) was observed for *Gossypium* spp., by Rebenfeld [3]. A similar decrease in tensile strength (σ_f) with microfibril angle has also been identified for wood fibres by Page *et al.* [4]. This similarity is utilized in addition to consideration for cellulose content (W_c) variation between species to show that there is a $\bar{\sigma}_f - \bar{E}$ correlation. This correlation is confirmed by results from an extensive analysis performed on fibres listed in categories I, II and V of Table I.

A physical cylindrical cell model (Fig. 1) is also utilized in obtaining a real representation of mean tensile strength by starting with the initial postulation that:

$$E_c = E_F \cos^2 \theta. \quad (1)$$

According to Treloar [5] this equation represents the axial Young's modulus, E_c , for a microfibril of Young's modulus, E_F , aligned at a filamentary winding angle, θ . The model is based on an extended analysis of cellulose content and average microfibril angle of some of the species tested; it is also shown to be applicable to previous measurements [6] for fibres in categories III and IV of Table I.

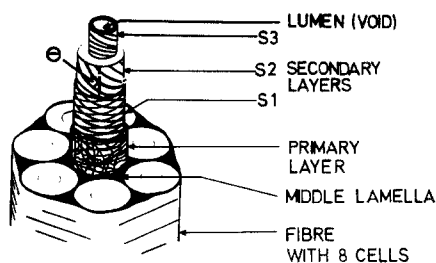


Figure 1 Cylindrical cell model of a plant fibre showing the lignified middle lamella region between cells, and the microfibril angle, θ , for the thick S2 layer of the predominantly cellulose walls.

TABLE I Five categories of cellulose fibres

Category	Examples
I. Leaf fibres	1. Sisal (<i>Agave sisalana</i> Perrine) 2. bowstring hemp (<i>Sansevieria metallica</i> Gérôme and Labroy) 3. – (<i>Cordyline fruticosa</i> L. A. Chev.) 4. gladiola (<i>Gladiolus X. hortuanus</i> V.) 5. raffia (<i>Raphia ruffia</i> Mart.)
II. Stem fibres	1. common bamboo (<i>Bambusa vulgaris</i> Schrad) 2. banana stalk (<i>Musa</i> spp.) 3. corn stalk (<i>Zea mays</i> L.) 4. – (<i>Eucalyptus</i> spp.) 5. pomegranate (<i>Punica granatum</i> L.) 6. bagasse (<i>Saccharum officinarum</i> L.) 7. coconut (<i>Cocos nucifera</i> L.)
III. Bast fibres	1. hemp (<i>Cannabis sativa</i> L.) 2. jutes (<i>Corchorus capsularis</i> and <i>C. olitorius</i> L.)
IV. Seed (-hair) fibres	1. cotton (<i>Gossypium</i> spp.)
V. Miscellaneous fibres	1. khuss khuss (<i>Vetiveria zizanioides</i> L. Nash) 2. guinea grass (<i>Panicum maximum</i> Jacq.) 3. coir (<i>Cocos nucifera</i> L.) 4. seymour grass (<i>Andropogon pertusus</i> L. Willd) 5. banana peel (<i>Musa</i> spp.) 6. hay grass (<i>Sporobolus</i> spp.) 7. pudding wythe (<i>Cissus sicyoides</i> L.) 8. coconut leaf sheath (<i>Cocos nucifera</i> L.) 9. cactus spine (<i>Cephalocereus swartzii</i> Griseb, Britton and Rose)

The present study was carried out to determine the best common empirical description of various plant species. The best empirical equations of mean tensile strength and mean fracture strain ($\bar{\epsilon}_f$) in terms of cellulose content and microfibril angle are also presented. By means of an extensive analysis performed on fibres which may be used in the production of synthetic materials, evidence for high works of fracture for different species is demonstrated in terms of a general fracture strain increase with increasing microfibril angle.

2. Experimental details

The fibres were extracted manually, using razor blades or scalpels where necessary. Care was taken at this stage not to damage the fibres through excessive straining. The mass of each fibre was measured using a microbalance. The cross-sectional dimensions were estimated by viewing the fibres in the transmitted light mode using an Olympus PME optical microscope. For this purpose, the image of a particular fibre was projected upon the ground glass screen of the microscope, so that the cross-sectional dimensions were directly measured using

a graticule superimposed upon that image. Most fibres were found to be approximately circular in cross-section and the associated area, A_m , was calculated upon the basis of a mean fibre diameter, \bar{d}_f .

A major problem, encountered in the tensile testing of small fibres, is the choice of a suitable gripping arrangement, which is both adequately stiff and yet does not damage the fibres. In the work described here, each fibre was first mounted upon a pair of brass studs and then held in place with epoxy glue. The mounted specimens were conditioned for 24 h at room temperature (24 to 27° C) in a desiccator maintained at 60% r.h. using a saturated solution of barium bromide. A sliver of bamboo attached to the studs, parallel to the specimen, facilitated careful transfer of the specimen and specimen mounts, from the conditioning rack to the locating holes. These holes were arranged to allow rotation of the studs so as to obviate eccentric loading on the specially constructed microtensometer described in Fig. 2. An extension rate of $16 \mu\text{m sec}^{-1}$ was employed and all tests were carried out at ambient conditions (26° C and 60% r.h. approximately). A continuous record of load versus deflection was made for each

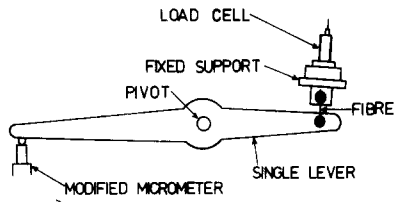


Figure 2 Fibre tensometer.

test. The fractured specimens were finally examined using the optical microscope as well as an ISI-60 scanning electron microscope (SEM).

The dry weight per cent of cellulose, W_c , was determined for a number of the fibre species, by using a process [7] in which 3 g portions to 40 to 60 mesh size sample were treated with 17.5% sodium hydroxide solution and washed with 10% acetic acid solution to remove other constituents. In addition, average microfibril filamentary winding angles for the S2 layers of individual species were estimated following the X-ray diffraction technique described by Preston [8].

3. Results and discussion

The fibres used consisted of bundles of single cells as is indicated by the diagram in Fig. 1. These cells contain a variety of layers which form a basically cylindrical arrangement, with the lumen space at the centre. This central lumen constitutes a reasonable fraction of the fibre cross-sectional area, as is shown in Fig. 3, and as such the measured cross-sectional area, A_m , based upon external dimensions, represents an over-estimate of the true cross-sectional area, A_t , which does not include the lumen space. The mean density of the cell-wall constituents has been estimated [9] to be of the order of $1.55 \times 10^3 \text{ kg m}^{-3}$. Using this

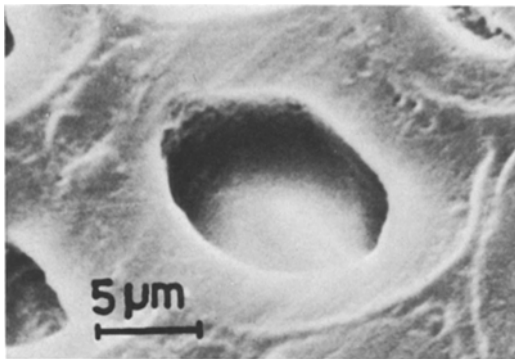


Figure 3 Scanning electron micrograph of bowstring hemp (*Sansevieria metallica*) fibre cell showing large central lumen.

figure, a reasonable approximation for the “true” cross-sectional area of a particular fibre, A_t , was given by

$$A_t = \frac{\rho_m A_m}{1.55 \times 10^3}, \quad (2)$$

where ρ_m is the measured fibre density.

Values of the fracture strength, σ_f , of each fibre as well as the corresponding axial Young’s modulus, E , were calculated on the basis of the “true” cross-sectional area according to the relationships:

$$\sigma_f = \frac{F_B}{A_t} \quad (3)$$

$$E = \frac{l_0}{A_t} \left(\frac{dF}{dl} \right)_{l=l_0}, \quad (4)$$

where F_B = breaking force, l_0 = initial gauge length, $(dF/dl)_{l=l_0}$ = slope of the load–extension response after allowance for machine stiffness has been made.

The absolute errors were about 10% for E and σ_f , about 5% for $\epsilon_f (= \Delta l/l \times 100\%)$, and about 1% for W_c and θ determinations.

The dependence of mechanical properties on cellulose content is confirmed by the non-zero correlation coefficients of $r = 0.538$ for E versus W_c , and $r = 0.749$ for E versus W_c , both at the 99.9% significance level: the results are illustrated by the plots in Fig. 4. These coefficients were obtained on a weighted basis without bias towards method of determination. These results, showing that both tensile strength and Young’s modulus increase with cellulose content, therefore provide a major reason for expecting a positive correlation between these two mechanical properties.

The additional increase in the two properties, tensile strength and Young’s modulus, with decreasing microfibril angle [3, 5] further contributed to the observation of a weighted correlation of $r = 0.689$ (at the 99.9% significance level) between $\bar{\sigma}_f$ and \bar{E} : This resulted in the following regression equation:

$$\sigma_f = 17.48 \times 10^{-9} E + 128.3 (\text{MN m}^{-2}) \quad (5)$$

which is superimposed over the plot of $\bar{\sigma}_f$ versus \bar{E} in Fig. 5, where each point represents the mean values of about five different observations. In this equation, which reflects the control of microfibril angle and cellulose content over a wide range of species, the mean Young’s modulus, \bar{E} , is given in N m^{-2} .

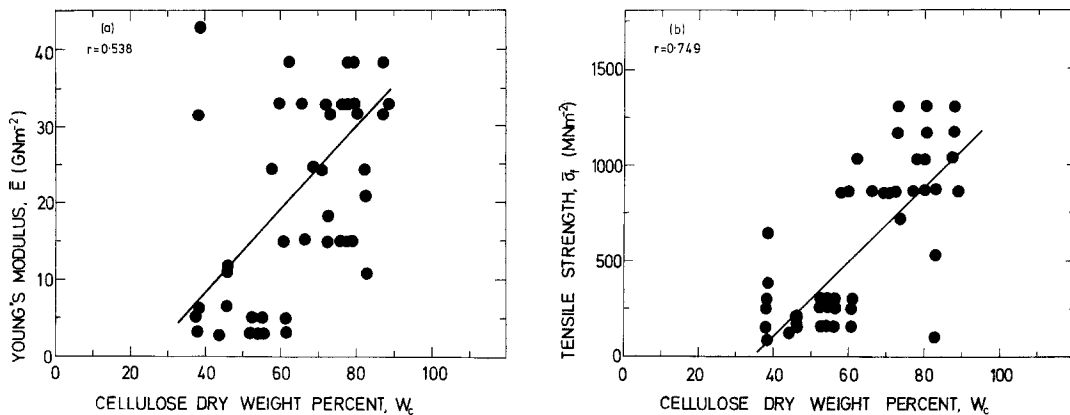


Figure 4 Plots of (a) mean Young's modulus, and (b) mean tensile strength, of various plant fibres versus cellulose dry weight per cent.

3.1. Cylindrical cell model

The physical cylindrical cell model is based on the following assumptions and approximations.

(i) The fibres contain continuous cylindrical cells which effectively reinforce the whole fibre in the same way that continuous fibres are understood to reinforce a conventional composite material.

(ii) The individual cells consist of several concentric layers, identified as the primary wall P , the outer secondary wall S_1 , the middle secondary wall S_2 and the inner secondary wall S_3 . However, the S_2 layer comprises such a large part of the cell wall material that the outer layers have an insignificant effect on the cell axial modulus.

(iii) The microfibrils of the S_2 layer trace a helix around the cell wall at an angle, θ , that is constant within the particular cell.

(iv) The cells which make up a particular fibre are treated as identical within that species.

Equation 1 is incorporated into a simple rule of mixtures approach to obtain the equation

$$\bar{E} = v_f E_f \cos^2 \theta + (1 - v_f) E_M, \quad (6)$$

where v_f is the volume fraction of the cellulose reinforcement, and E_M represents the Young's modulus of the matrix. Substitution of this representation of \bar{E} into Equation 5 produces the following equation for strength:

$$\bar{\sigma}_f = 17.48 \times 10^{-9} v_f E_F \cos^2 \theta + 17.48 \times 10^{-9} (1 - v_f) E_M + 128.3 (\text{MN m}^{-2}). \quad (7)$$

This representation is rewritten in the form:

$$\frac{\bar{\sigma}_f - 128.3}{1 - v_f} = \frac{17.48 \times 10^{-9} v_f E_F \cos^2 \theta}{1 - v_f} + 17.48 \times 10^{-9} E_M, \quad (8)$$

where $\bar{\sigma}_f$ is in MN m^{-2} so that E_F and E_M are obtained from a regression of $(\bar{\sigma}_f - 128.3) \div (1 - v_f)$ against $v_f \cos^2 \theta \div (1 - v_f)$.

Mathematical analysis was performed using various deduced values of v_f . This process utilized the densities of the cellulose microfibrils and other components of the tissue which lie in the narrow range of 1.4 to $1.6 \times 10^3 \text{ kg m}^{-3}$ [10, 11]. Density contribution was therefore such that v_f could be replaced by the weight fraction of cellulose, $W_c \div 100$. As a result, Equation 8 is rewritten as:

$$\frac{\bar{\sigma}_f - 128.3}{100 - W_c} = \frac{N_1 W_c \cos^2 \theta}{100 - W_c} + N_2 \quad (9)$$

where $\bar{\sigma}_f$ is kept in MN m^{-2} . The constants N_1 and

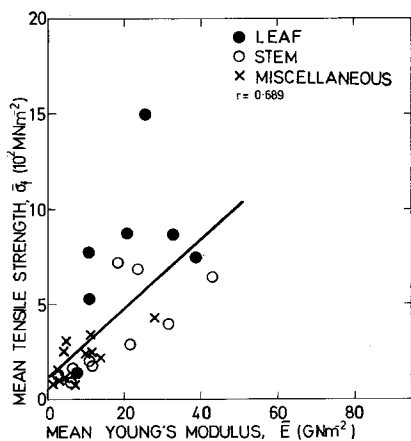


Figure 5 Mean tensile strength of various plant fibres plotted against Young's modulus showing a positive correlation.

N_2 are proportional to E_f and E_M , respectively, and are obtained by regression. The results used for this purpose were those of fibres from the three categories analysed for which, in addition to the mechanical properties, the cellulose content and the microfibril angles were determined. An evaluation of the equation is illustrated in Fig. 6 where the individual calculated values of $(\bar{\sigma}_f - 128.3) \div (100 - W_c)$ is plotted against $W_c \cos^2 \theta \div (100 - W_c)$ on which the regression line is superimposed.

The correlation coefficient for $(\bar{\sigma}_f - 128.3) \div (100 - W_c)$ against $W_c \cos^2 \theta \div (100 - W_c)$ is 0.901 at the 99.9% significance level for results obtained in our UWI laboratory. When previous measurements [6] are added $r = 0.925$, using median values of σ_f and θ in cases where only maximum and minimum values are available. The Young's modulus of the matrix deduced from the regression line is $E_M = 0.34 \text{ GN m}^{-2}$, with a standard error of 3.1 GN m^{-2} , compared to 2 GN m^{-2} , the Young's modulus of lignin [12, 13]. A result of 3.4 GN m^{-2} is obtained when the standard error is added to the predicted low E_M value, and this figure is a good indication of the maximum matrix modulus. Therefore, the calculated results seem to be reasonable, especially because of the following reasons: (1) E_M is combined with a much higher E_F value which should affect the inaccuracy of E_M predictions; (2) the standard error associated with an E_M prediction should be relatively high, since it must account for the natural variations in matrix properties between the various species. The deduced value of the microfibril Young's modulus is $E_F = 45.0 \text{ GN m}^{-2}$, with a standard error of 0.8 GN m^{-2} , compared to

56.5 GN m^{-2} which was calculated theoretically by Treloar [14] and by Jawson *et al.* [15].

The resulting representation of mean tensile strength included an initial correlation coefficient of $r = 0.790$ between predicted and measured results.

3.2. Empirical equations

An improvement in the prediction for mean tensile strength is given by the best fit which was obtained from a regression of $\bar{\sigma}_f$ against $W_c \cos^2 \theta$ and $W_c(\cos \theta - \sin \theta) \sin \theta$ giving $r = 0.892$ at the 99.9% significance level. As is expected from inspection of the model the $W_c \cos^2$ term is most dominant since the empirical equation is:

$$\bar{\sigma}_f = 14.9 W_c \cos^2 \theta - 60.9 W_c (\cos \theta - \sin \theta) \sin \theta + 240 (\text{MN m}^{-2}). \quad (10)$$

The possibility of obtaining strain interaction between the microfibrils (across the matrix) is a likely reason for the requirement of the modified terms which are presented in Equation 10 as compared to the results derived from the model, and which are represented by Equation 7. An evaluation of Equation 10 is shown in Fig. 7.

In addition, a detailed analysis revealed that the control of W_c over $\bar{\sigma}_f$ is not reflected on fracture strain, ϵ_f , which is more dependent on θ . While the $\bar{\epsilon}_f - W_c$ correlation coefficient is 0.00 there is general parabolic fracture strain—microfibril angle relationship represented by the regression equation:

$$\bar{\epsilon}_f = 1.30 + 9.96 \times 10^{-3} \theta^2 (\%) \quad (11)$$

for θ in degrees.

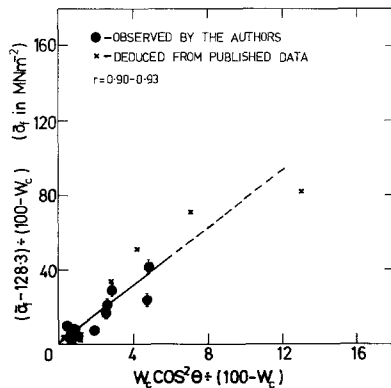


Figure 6 Evaluation of cylindrical cell model by a plot of measured results, on which the weighted regression line is superimposed.

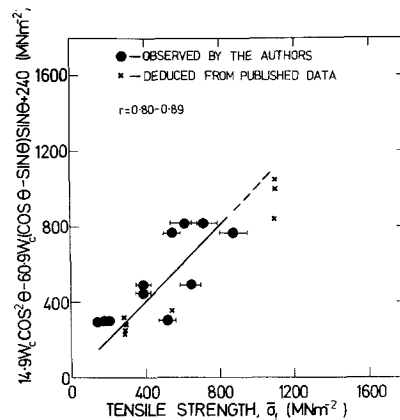


Figure 7 Predictions from the empirical equation plotted against measured mean tensile strengths for various species of natural fibres.

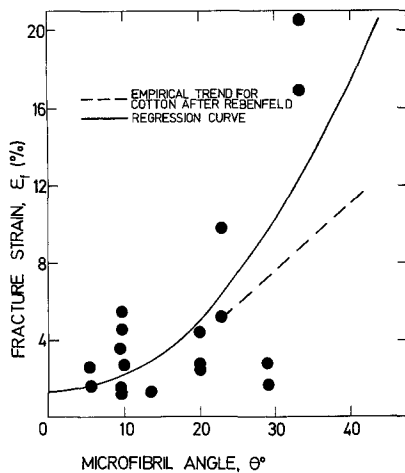


Figure 8 Mean fracture strains plotted against average microfibril angle, on which a parabolic regression curve giving a correlation coefficient of $r = 0.691$ between predicted and measured results is superimposed.

The curve described by this equation is superimposed on the plotted results for mean fracture strain versus average microfibril angle in Fig. 8. The empirical trend for cotton (*Gossypium* spp.) [3] is also illustrated. The contribution of microfibril angle to increasing fracture strain provides direct evidence for the high works of fracture, which will even be greater for high strain fibres as a natural consequence of microfibril uncoiling that is necessarily increased at larger angles.

The failure of various species of cellulosic fibres which is therefore subjected to a common control by cellulose content and microfibril angle, is presently described in Fig. 9 for the leaf fibre bowstring hemp (*Sansevieria metallica*), and two miscellaneous fibres coir (*Cocos nucifera* L.) and pudding wythe (*Cissus sicyoides*). These fibres failed in tension, as is expected from the model, by fracture at the cell walls with delamination and uncoiling of the microfibrils. Thus microscopy revealed that instead of shearing out at their ends, the cells failed for the most part with the fracture of the cell walls. Fig. 9a shows some degree of buckling for two cells which protrude from the greater part, which failed sharply and approximately at right angles to the axis of the described low-strain bowstring hemp specimen. Fig. 9c shows a pudding wythe specimen (including thin-walled broad cells) which has medium values of fracture strain: $\bar{\epsilon}_f \doteq 15\%$. For this second species the effect of cell wall buckling and delamination is

greater than for the low-strain species, bowstring hemp. Fig. 9b shows the gross degree of uncoiling obtained for the very high-strain (narrow cell) coir species. The bowstring hemp fibres which were observed to demonstrate low fracture strains for the most part in the range 3 to 6% also had a lower average microfibril angle of 9.4° which is consistent with its relatively low degree of uncoiling (Fig. 9a). At the other extreme, the coir fibres with high microfibril angles in the range 30 to 35° were observed to fail with very high strains of 15 to 30%. In particular, coir fibres fail with the simultaneous uncoiling of the microfibrils in the walls of adjacent cells (Fig. 9b).

The present results, therefore, provide evidence in support of the greater degree of uncoiling within the cell walls due to the increasing microfibril angle, θ , which increases the maximum strain that is obtained. Thus it is shown that θ is an extremely significant factor in predicting the behaviour of cellulosic fibres under axially applied tensile stresses. By increasing the fracture strains this factor serves to increase the area under the stress versus strain curves. It also follows as a direct consequence from this latter effect that high works of fracture can be achieved, and have been previously reported [1, 2]. Thus whereas large cellulose content contributes to increasing the tensile strengths, the fracture mechanism of the various plant species is such that the larger microfibril angles (regardless of their association with lower strengths) contribute to the development of large works of fracture.

4. Conclusions

(1) A positive correlation between mean tensile strength and mean Young's modulus is explained by the increase in both properties with increasing cellulose content and decreasing microfibril angle for a wide variety of plant fibres.

(2) The development of a cylindrical cell model has assisted in establishing a major dependence of mean tensile strength on the product of cellulose dry weight per cent and the square of the cosine of the microfibril winding angle.

(3) The increase in mean fracture strain with average microfibril angle for various plant fibres provides further evidence of the high works of fracture. These high works of fracture can be obtained because of the uncoiling of the cellulose microfibrils in response to axial application of tensile stresses.

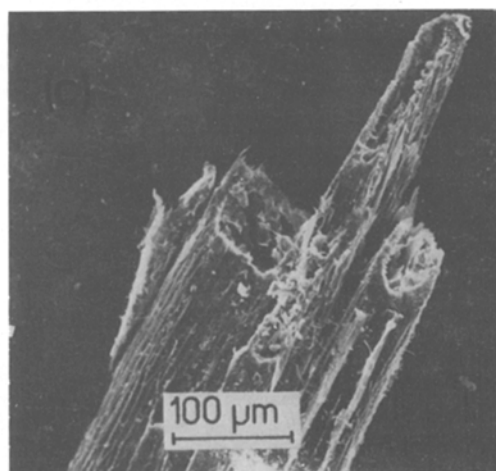
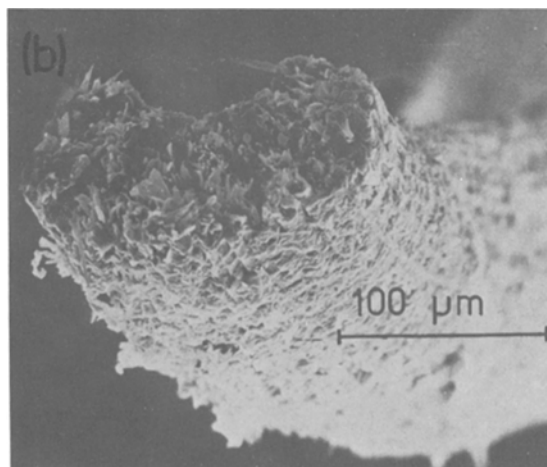
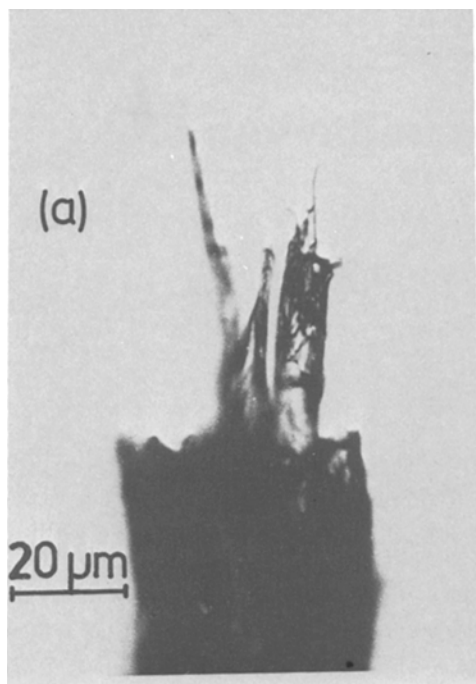


Figure 9 Micrograph showing examples of delamination and uncoiling in the failure zones of plant fibres fractured in tension: (a) bowstring hemp (*Sansevieria metallica*), (b) coir (*Cocus nucifera* L.), and (c) pudding wythe (*Cissus sicyoides* L.).

Acknowledgement

Some data on cellulose content were obtained from the Tropical Products Institute, UK.

References

1. G. JERONIMIDES, Leiden Botanical Series No. 3 (1976) p. 253.
2. E. C. MCLAUGHLIN and R. A. TAIT, *J. Mater. Sci.* **14** (1979) 998.
3. L. J. REBENFELD, *J. Pot. Sci. C.* **9** (1965) 91.
4. D. H. PAGE, F. EL-HOSSEINY, K. WINKLER and R. BAIN, Canadian Pulp and Paper Association – Meetings of the Technical Section, August (1972) T198.
5. L. R. G. TRELOAR, *Physics Today*, December (1977) 23.
6. A. FREY-WYSSLING, “The Plant Cell Wall” (Gebrüder Bornbraegar, Berlin, 1976) p. 217.
7. J. GRANT, “A Laboratory Handbook of Pulp and Paper Manufacture”, 2nd Edn (Edward Arnold, London, 1961) p. 131.
8. R. D. PRESTON, “The Molecular Architecture of Plant Cell Walls” (Chapman and Hall, London, 1952) pp. 40, 120.
9. L. HOLLIDAY, “Composite Materials”, (Elsevier, Amsterdam, 1966) p. 486.
10. R. E. MARK, “Cell Wall Mechanics of Tracheids” (Yale University Press, New Haven, 1967) p. 107.
11. R. D. PRESTON, “The Physical Biology of Plant Cell Walls” (Chapman and Hall, London, 1974) p. 376.
12. R. E. MARK, “Cell Wall Mechanics of Tracheids” (Yale University Press, New Haven, 1967) p. 144.
13. P. S. SRINIVASAN, *Quart. J. Indian Inst. Sci.* **4** (2) (1941) 222.
14. L. R. G. TRELOAR, *Polymer* **1** (1960) 290.
15. M. A. JAWSON, P. P. GILLIS and R. E. MARK, *Proc. Roy. Soc. A* **306** (1968) 389.

Received 13 March and accepted 28 June 1979.